Exposure-based smart ventilation and occupancy control for optimizing ventilation energy consumption and long-range airborne transmission of COVID-19 in school environments

https://doi.org/10.1007/s12273-025-1292-0

Exposure-based smart ventilation and occupancy control for optimizing ventilation energy consumption and long-range airborne transmission of COVID-19 in school environments

Xiaowei Lyu[1], Zhiwen Luo[2,3] (✉), Emmanuel Essah[1], Zhan Shu[4], Li Shao[1]

1. School of the Built Environment, University of Reading, Reading, UK
2. School of Public Health, Zhengzhou University, Zhengzhou, China
3. Welsh School of Architecture, Cardiff University, Cardiff, UK
4. Department of Electrical and Computer Engineering, University of Alberta, Edmonton, Canada

Abstract

Mechanical ventilation is an effective measure to control indoor long-range airborne transmission of COVID-19, but it often leads to substantial energy expenditure. This study introduces a novel exposure-based smart ventilation and occupancy control strategy to reduce infection risk and save energy in school environments that are typically characterized by fixed occupants and long exposure time. This exposure-based approach allows the quanta concentration to vary over time rather than keeping it constantly below certain thresholds. This enables us to: (1) adjust ventilation and occupant schedule to facilitate passive cooling/heating potential in response to outdoor weather conditions; (2) consider the interaction between ventilation and occupant schedule to maximize their benefits in reducing infection risk and energy consumption. Taking a typical classroom as a base case, ventilation and occupant schedule are optimized individually and jointly through Genetic Algorithm, to control infection risk, minimize energy consumption, maintain thermal comfort, and promise sufficient schooling time. Our results show that the most energy-efficient strategy is the concurrent optimization of both occupant schedule and ventilation, achieving an energy reduction of up to ~60% compared to traditional constant ventilation methods. Solely optimizing occupant schedule is the least energy-efficient strategy, yielding an energy reduction ratio (over base case) of only half of the most efficient strategy. Our study reveals the possibility of optimizing occupant schedule and ventilation to balance building energy consumption and transmission control. The viability of these control strategies has been proven across various climate zones and seasons in China, highlighting their broad applicability.

Keywords

airborne transmission
building control
smart ventilation
intermittent occupancy

Article History

Received: 29 December 2024
Revised: 21 March 2025
Accepted: 11 April 2025

1 Introduction

Long-range airborne transmission specifically refers to the inhalation of infectious aerosols from room air at a distance of larger than ~1–2 m from the infector (Wei and Li 2016; Li 2021). Numerous outbreaks of severe respiratory diseases, such as COVID-19, have been proven to be induced by this transmission route in poorly ventilated spaces (Buonanno et al. 2020a; Li et al. 2021; Miller et al. 2021). Controlling long-range airborne transmission in school-like environments is critical, as students typically remain in the same environment for extended periods. Moreover, maintaining proper masking and distancing measures can be challenging for young children, thus increasing the long-range airborne transmission risk compared to other indoor settings.

Increasing outdoor ventilation is a recommended strategy to reduce long-range airborne transmission indoors (Buonomano et al. 2023; Pang et al. 2023; Morawska et al. 2024), but it can also substantially increase building energy consumption (Zheng et al. 2021; Pang et al. 2023). Developing ventilation strategies that effectively balance transmission control with energy efficiency in school-like environments

E-mail: LuoZ18@Cardiff.ac.uk

is crucial. In fact, various energy-efficient ventilation strategies have been proposed to control long-range airborne transmission by dynamically adjusting ventilation. However, these ventilation control strategies are not well-suited for school-like environments. First, current dynamic ventilation schemes typically adjust ventilation rates based on varying occupancy levels (Sha et al. 2021; Zhuang et al. 2022; Wei et al. 2023; Li et al. 2024) or the corresponding CO_2 concentration, which is primarily influenced by occupancy levels (Li and Cai 2022; Risbeck et al. 2023). This approach is ineffective for spaces with fixed occupancy, such as schools, where the required ventilation remains constant. Second, most of these ventilation strategies aim to constrain quanta concentration consistently below a predefined threshold (corresponding to a risk limit) for transmission control (Sha et al. 2021; Li and Cai 2022; Zhuang et al. 2022; Wei et al. 2023), clarifying them as concentration-based control strategies. However, in school-like environments, concentration-based ventilation control can lead to both a constant (due to the fixed occupancy) and high (due to the extended exposure time) ventilation demand, leading to substantial increase of building energy consumption (Melikov et al. 2020; Zhang et al. 2021). Consequently, new ventilation strategies are required to control transmission effectively in school settings while maintaining energy efficiency.

Some studies have proposed implementing intermittent occupancy to address the challenge of high ventilation demand in school-like environments for infection risk control (Melikov et al. 2020; Zhang et al. 2021, 2023c). By leveraging the natural decay of quanta concentrations during unoccupied periods, intermittent occupancy strategies can reduce the need for continuous outdoor air ventilation while mitigating transmission risk (Zhang et al. 2021, 2023c). However, existing intermittent occupancy strategies have been developed based on constant ventilation schemes, and their energy-saving potential remains largely unexplored. Given that ventilation and occupancy are two key factors influencing both transmission risk and energy consumption (Zhang et al. 2023b), optimizing them either individually or jointly could help minimize energy use while maintaining effective transmission control. Further research is needed to explore this potential.

This study aims to develop an exposure-based control theory to regulate both ventilation and occupancy for efficiently managing airborne transmission while minimizing energy consumption in school-like environments. Unlike traditional concentration-based control strategies, which constrain instantaneous quanta concentrations below a fixed threshold, our exposure-based approach regulates time-integrated quanta concentration (quanta exposure) for transmission control, allowing quanta concentrations to fluctuate dynamically over time. This flexibility enables ventilation and occupant schedules to be adjusted in response to outdoor weather conditions to enhance energy efficiency. For example, during periods of high heating or cooling demands due to outdoor ventilation, ventilation rates can be strategically decreased to permit higher quanta concentration, and conversely increased during periods of lower demand, ensuring that the overall virus exposure remains within controlled limits. Compared to conventional dynamic ventilation strategies, which adjust ventilation based on occupancy variations, our exposure-based control strategy enables ventilation adjustments based on outdoor weather conditions, making it more suitable for exploring energy-saving opportunities in spaces with fixed occupancy. By leveraging this approach, the energy-saving potential of both occupancy adjustments and ventilation strategies can be further explored.

In Section 2, four different optimization strategies are detailed, i.e., optimizing ventilation only, optimizing occupant density only, optimizing both ventilation and occupant schedule consistently and dynamically. In Section 3, we demonstrated the effectiveness of these strategies using a typical classroom scenario. The mechanisms of how each strategy reduces energy consumption while managing the risk of airborne infection have also been analyzed in this section. Our research highlights the potential of these optimized strategies to revolutionize indoor air management, balancing the imperative concern of health safety with the need for environmental sustainability.

2 Methodology

Our control strategy is specifically designed for school environments that rely solely on mechanical ventilation systems all the time, excluding natural ventilation (Sha et al. 2021; Guo et al. 2022). It operates on the premise that classroom occupancy corresponds with the school schedule, including both class and break segments. We assume that classrooms will be completely unoccupied during break segments, thereby establishing an intermittent occupant schedule.

2.1 School environment base case study

A typical classroom is adopted for our case study (Peng and Jimenez 2021), with specific parameter to be found in Table 1. Given that occupants—including students and teachers—are typically seated or standing during class periods, we assume they engage primarily in sedentary activities, corresponding to a breathing rate of 0.54 m^3/h (Adams 1993). Additionally, we adopted a worst-case scenario by assuming the indoor infectious individual is the

Table 1 Basic parameters for case study

Parameters	Volume [m^3]	Occupants	Infectors	Activity-respiratory	Quanta emission rate [quanta/h]	Breathing rate [m^3/h]	Schedule duration
Values	142	10	1	Sedentary-speaking	1.7	0.54	9:00–16:00

teacher, who typically speaks during classes, thereby generating a higher quanta emission rate compared to quiet breathing (Peng and Jimenez 2021). Consequently, the quanta emission rate was estimated to be 1.7 quanta/h, calculated by multiplying the baseline emission rate for sedentary breathing (0.37 quanta/h) (Buonanno et al. 2020a) by a relative quanta emission factor of 4.7. This factor captures the combined effects of increased respiratory activity and vocalization associated with teaching activities (Peng et al. 2022).

Figure 1 explains the base case scenario. It features red columns representing occupancy segments and green columns for break segments (including lunch break at 11:45–13:00). The width of these columns indicates the duration of each segment, while their height reflects the air change rate (ACH) during those segments. The total occupancy period spans from 9:00 to 16:00, adhering to a standard classroom schedule that includes 0.75 h class time and 0.25 h break time, along with a 1.25 h lunch break commencing at 11:45. The ACH is maintained constant throughout the occupant schedule at approximately 2 ACH. Notably, this ventilation rate is determined for controlling the infection risk below 1%, by limiting the time-integrated quanta exposure during all the occupancy segments (refers to Section 2.4). In accordance with the occupant schedule and ventilation of the base case, the quanta concentration—depicted by the blue line in the figure—changes between rising during occupancy segments and falling during break segments (the calculation of quanta concentration can be found in Section 2.3).

2.2 Optimization strategies

The exposure-based infection risk control theory focuses on limiting total virus exposure rather than just the quanta

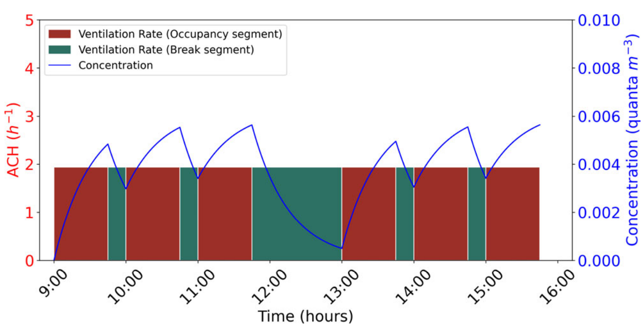

Fig. 1 Quanta concentration variation in the base case scenario based on constant ACH and fixed occupant schedule

concentration to manage infection risks, which allows for adjustments in the timing of occupant schedules as well as the value of air change rate (ACH) during each time segment. This offers a practical method to balance the reduction of infection risks with energy savings by (1) adapting ventilation and occupant schedule to external weather conditions for maximizing passive heating/cooling potential; and (2) considering the interaction between ventilation and occupant schedule, thereby maximizing their benefits in lowering both energy consumption and infection risk.

Building upon the exposure-based control principles, our research introduces four distinct optimization strategies in response to different levels of system complexity. These strategies employ different approaches to manage ventilation systems and occupant schedules, either individually or in combination, to explore energy conservation potentials in controlling airborne transmission.

Strategy 1 - Ventilation only: This strategy focuses solely on optimizing the ACH during each time segment, while the occupant schedule (including occupancy and break segments) remains unchanged from the baseline.

Strategy 2 - Occupant schedule only: Contrary to Strategy 1, this approach optimizes only the occupant schedule. The optimal duration of occupancy segments and break segments vary over time, but the total accumulated occupancy time remains equal to the base case. The ACH is kept constant across all segments as in the baseline scenario.

Strategy 3 - Consistent ventilation and occupant schedule: This strategy focuses on optimizing both the occupant schedule and the ACH at the same time. However, it optimizes the occupant schedule in a consistent manner across all the segments to minimize the disruption to the learning, meaning all optimal occupancy segments have the same duration, and all break segments (except lunch break) also have a uniform length (easy to be implemented in the timetable). Similarly, the ACH are set to be consistent within their respective segments; the rate is the same during all occupancy segments and uniform across all break segments (except lunch break). the total cumulative occupancy time is consistent with the base case.

Strategy 4 - Flexible ventilation and occupant schedule: This strategy offers the most comprehensive approach to optimize both the occupant schedule and ventilation. It stands out from Strategy 3 by allowing the duration of occupancy and break segments, as well as the ACH during each segment, to vary throughout the designated time zone (9:00–16:00). Likewise, the total cumulative occupancy duration is identical to the baseline scenario.

The four optimal strategies are implemented in four representative cities located in different climate zones: Harbin from the very cold climate zone, Beijing from the cold zone, Shanghai from cold winter and hot summer zone, and Guangzhou from the warm winter and hot summer zone. The outdoor weather conditions for these cities, such as temperature and relative humidity, come from the Typical Meteorological Year (TMY) dataset found in EnergyPlus weather data (https://energyplus.net/weather).

Ventilation and occupant schedules are optimized on a daily basis, but our analysis encompasses all four seasons, with five consecutive days selected to represent 5 schooling days: March 20–24 for spring, June 21–25 for summer, September 23–27 for autumn, and December 21–25 for winter. The optimization mechanisms of each strategy are illustrated using the results from a typical winter day in Harbin (see Section 3.1). Then, the total energy consumption over five school days is also analyzed to assess the energy-saving potential of the strategies across various climates (see Section 3.2).

2.3 Modelling

2.3.1 *Long-range airborne transmission model*

Indoor long-range airborne transmission risk P is modelled through the Wells–Riley equation (Riley et al. 1978):

$$P = 1 - \mathrm{e}^{-n_{\mathrm{q}}} \tag{1}$$

where n_{q} is the total inhaled quanta quantity.

According to the study of Lyu et al. (2023), for spaces with fixed occupants, the total inhaled quanta quantity n_{q} can be expressed as:

$$n_{\mathrm{q}} = \sum_{i=1}^{n_{\mathrm{o}}} \int_0^{T_i} B C_{\mathrm{q},i}(t)\,\mathrm{d}t \tag{2}$$

The occupant schedule encompasses both occupancy and break segments. In this context, i only represents the ith occupancy segment, while n_{o} represents the number of total occupancy segments. T_i and $C_{\mathrm{q},i}$ are the occupancy time duration, h, and instant quanta concentration, quanta/m^3, corresponding to the ith occupancy segment, respectively. B is the breathing rate, m^3/h.

The variations of quanta concentration during segment i (either occupancy or break segment) is modelled by mass balance equation based on well mixed assumption and can be expressed as:

$$\frac{\mathrm{d}C_{\mathrm{q},i}}{\mathrm{d}t} = \frac{I_i E_{\mathrm{q}}}{V} - \lambda_i C_{\mathrm{q},i} \tag{3}$$

$$C_{\mathrm{q},i}(t) = \left(C_{\mathrm{qin},i} - \frac{I_i E_{\mathrm{q}}}{\lambda_i V} \right) \mathrm{e}^{-\lambda_i t} + \frac{I_i E_{\mathrm{q}}}{\lambda_i V} \tag{4}$$

where V is the space volume, m^3; λ_i is outdoor air change rate during segment i, h^{-1}; E_{q} is quanta emission of infector, quanta/h; $C_{\mathrm{qin},i}$ is initial quanta concentration for segment i, quanta/m^3; I_i is infector number, and it is equal to 1 for occupancy segment and 0 for break segment.

Notably, our study considered only long-range airborne transmission. However, recent studies have introduced a new modelling approach that links short- and long-range airborne transmission (Feng et al. 2024; Henriques et al. 2025). This approach could be integrated into our exposure-based control theory in future research to develop more effective occupancy and ventilation control strategies, accounting for the continuity of airborne transmission.

2.3.2 *Ventilation energy consumption model*

Given that long-range airborne transmission is notably influenced by outdoor ventilation, it is crucial to quantify the relationship between infection risk and energy consumption attributed to outdoor ventilation. Outdoor ventilation energy consumption mainly includes two parts, the energy consumption of ventilation fan (E_{fan}), and the heating/cooling load due to outdoor ventilation ($E_{\text{AC-load}}$).

The heating/cooling load due to outdoor ventilation in stage i, $E_{\mathrm{AC},i}$, can be expressed as Equation (5) (Guo et al. 2022):

$$E_{\text{AC-load},i} = \int_0^{T_i} \rho_{\mathrm{a}} \lambda_i V \left(\frac{\Delta h^{\mathrm{h}}}{\mathrm{COP_h}} - \frac{\Delta h^{\mathrm{c}}}{\mathrm{COP_c}} \right) \mathrm{d}t \tag{5}$$

where ρ_{a} is the density of air, 1.293 kg/m^3; $\mathrm{COP_h}$ (3.5) and $\mathrm{COP_c}$ (3.0) are coefficient of heating and cooling performance, respectively (Guo et al. 2022); Δh^{h} and Δh^{c} refer to the indoor-outdoor enthalpy difference in heating and cooling mode, respectively.

The enthalpy (h) can be calculated using Equation (6) (Guo et al. 2022):

$$h = 1.005 T_{\mathrm{e}} + w(2500 + 1.84 T_{\mathrm{e}}) \tag{6}$$

where T_{e} is the dry-bulb temperature, °C, and w is air moisture, g/kg; w is calculated as (Nie et al. 2018):

$$w = 0.622(2500 + 1.84 T_{\mathrm{e}}) \frac{0.01\mathrm{RH}\,\mathrm{e}^{23.58 - 4043/(T_{\mathrm{e}} + 273.15 - 37.58)}}{P_0 - 0.01\mathrm{RH}\,\mathrm{e}^{23.58 - 4043/(T_{\mathrm{e}} + 273.15 - 37.58)}} \tag{7}$$

where RH is relative humidity, %; P_0 is the barometric pressure of the air, Pa.

A simplified fan power energy consumption is expressed as below based on an assumption of 1 kW/(m^3·s) specific fan power (SFP) for ventilation system without heat recovery (Guo et al. 2022):

$$E_{\mathrm{fan},i} = \int_0^{T_i} \mathrm{SFP} \cdot \lambda_i V \mathrm{d}t \tag{8}$$

The total energy consumption of the interesting time duration can then be expressed as:

$$E_{\mathrm{total}} = \sum_{i=1}^{n_o+n_b} \left(E_{\mathrm{fan},i} + E_{\mathrm{AC\text{-}load},i} \right) \tag{9}$$

here n_b refers to total number of break segments.

2.4 Optimization algorithm

Our study includes four primary objectives: maintaining indoor thermal comfort, limiting infection risk, ensuring sufficient schooling time, and minimizing energy consumption. The main objective functions are shown in Equations (10)–(14). To ensure satisfied indoor thermal environment, the indoor temperature and relative humidity (RH) are set to be between 20–25 °C and 40%–50% (Equations (10) and (11)), respectively (Guo et al. 2022). The determination of indoor infection risk threshold is important for both infection risk control and energy consumption reduction, considering that a high-risk threshold (P_t) may not ensure a safe indoor environment, while setting it too low could lead to excessive energy consumption due to the increased required ventilation. However, it is not a trivial task to identify a one-size-fit-all threshold. While previous studies have adopted different risk thresholds, ranging from 0.01% to 1% (Dai and Zhao 2020; Peng and Jimenez 2021), we set the infection risk threshold at 1% in this study because this level is sufficiently low to keep the event reproduction number (R_{event}) below 1 for the classroom with 10 occupants while being high enough to prevent unnecessary energy use (Bazant and Bush 2021). However, it should be noted that a 1% risk threshold may be unsafe in classrooms with more than 100 occupants. Based on this threshold, we can then determine the appropriate quanta exposure limit for the entire occupancy period (Equation (12)). To guarantee adequate study time, the total occupancy duration in the optimization is set to match the total class time in the base case, equaling to 0.75 × 6 h per day (Equation (13)). The overall schedule duration is strictly constrained to match the base case schedule, which is from 9:00 to 16:00.

In order to generate viable solutions for the optimization problem, establishing search ranges for the key decision variables is essential. To derive practical durations for the occupant schedule, specified search ranges for class time, break time, and lunch break have been determined. Specifically, class time is set to range from 0.5 to 1.5 h, break time (except lunch break) from 0.1 to 0.5 h, and the minimum duration for lunch break is established at 0.70 h. This ensures class periods are not too long, and breaks are not too short.

$$20\ ^\circ\mathrm{C} \le T_e \le 25\ ^\circ\mathrm{C} \tag{10}$$

$$40\% \le \mathrm{RH} \le 50\% \tag{11}$$

$$n_q \le -\ln(1 - P_t) \tag{12}$$

$$\sum_{i=1}^{n_o} T_i \ge 4.5 \tag{13}$$

$$\mathrm{Min}\ E_{\mathrm{total}} \tag{14}$$

Genetic Algorithm (GA) is employed to address the optimization problem, which is a heuristic search that emulates Charles Darwin's theory of natural selection, incorporating processes such as crossover, mutation, and selection. Figure 2 shows the whole optimization process in detail, using Strategy 4 as an example. In Strategy 4, the key

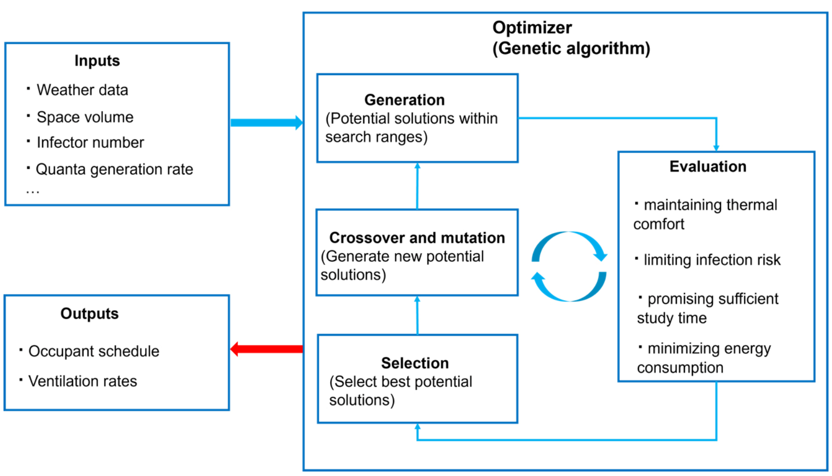

Fig. 2 Overall optimization process (taking Strategy 4 for example)

decision variables include the occupant schedule (covering all occupancy and break segments including lunch break) and the ACH for each segment. In summary, the optimization process can be broken down into generation, evaluation, selection, crossover, and mutation phases. For each iteration of the algorithm, we generate a population of 2000 solutions within the defined search ranges for the decision variables. These solutions are then evaluated against our main objectives. The best performing solutions are selected and undergo crossover and mutation, creating another 2000 solutions for the next cycle. Over time, the solutions improve, shown by smaller increases in the evaluation scores. If there is less than a 0.1 improvement over 100 consecutive cycles, we consider the best current solution as the optimal one.

Critical parameters in GA, such as crossover probability, mutation probability, population size, generation numbers (or stopping criteria), and the selection method, require precise tuning for efficient and accurate problem-solving. The optimal values for these parameters or the most appropriate selection method depend significantly on the specific nature of the optimization problem and the characteristics of the decision variables (Mokhtari and Jahangir 2021). In our study, we started with empirical defaults based on a literature review of similar research questions (Mokhtari and Jahangir 2021; Zhang et al. 2021) and then conducted a sensitivity analysis to identify the suitable hyperparameters that balance exploration and exploitation. Specifically, we investigated how the different hyperparameter settings impact the simulation accuracy and computation efficiency by running multiple simulations. The sensitivity analysis for Strategy 4 is demonstrated in the Supplementary Material. The final hyperparameters were selected based on achieving high simulation efficiency while maintaining acceptable accuracy, as was shown in Table 2.

Table 2 Parameters for the optimization algorithm

Parameter	Value
Crossover probability	20%
Mutation probability	70%
Population size	2000
Stopping criteria	Improvement less than 0.1 for 100 generations
Selection method	Tournament with tour size = 2

3 Results and discussion

3.1 Comparing different strategies

In this section, we compare the four proposed strategies, using a specific day for example. Given our optimization is based on daily data, it is important to note that the optimal solutions can vary from day to day, influenced by the changing patterns of outdoor weather conditions across different days, seasons, and cities. We chose December 21st in Harbin during winter as a case to illustrate the results of different strategies. This selection is mainly due to the significant variations in outdoor weather conditions on that day, which highlights the energy-saving potential of our optimization strategies.

Figure 3 displays the outdoor weather conditions, including temperature and relative humidity, for the selected day during the schooling period, while Figure 4 presents the

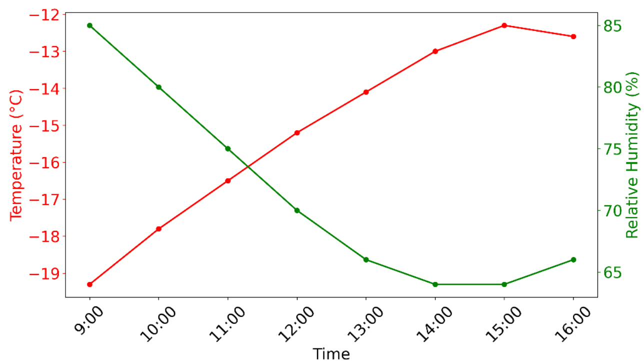

Fig. 3 Outdoor weather conditions, including temperature and relative humidity on a specific day (December 21st) during the winter in Harbin

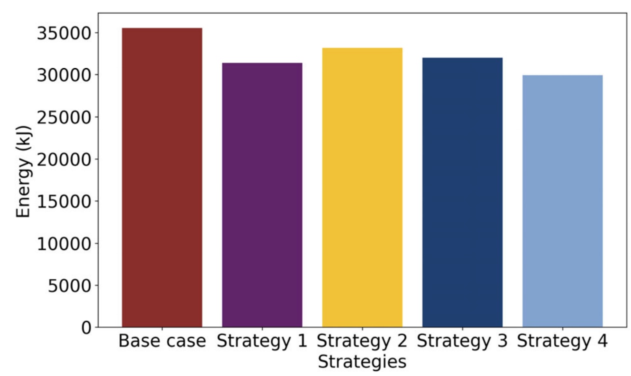

(a)

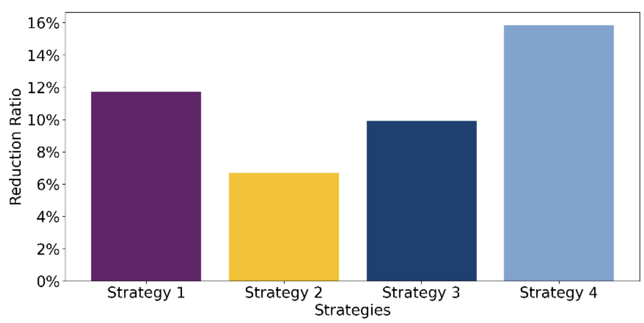

(b)

Fig. 4 The (a) energy consumption and (b) energy reduction ratio compared to the base case for various strategies on a specific day (December 21st) during the winter in Harbin energy consumption and the energy reduction ratio compared to the base case for the evaluated strategies. Notably, all four strategies in Figure 4 result in the same virus exposure for occupants that corresponds to an infection risk of 1%. The findings reveal that Strategy 4 emerges as the most energy-efficient strategy, realizing an estimated energy reduction of approximately 16%, more than twice as high as Strategy 2 (7%). Strategy 1 (12%) and Strategy 3 (10%) are the second and third most energy-efficient strategies, respectively. The subsequent sections will delve into the detailed outcomes and further explore the potential mechanisms behind the energy savings achieved by these strategies.

3.1.1 Strategy 1 - constant occupant schedule but varying ventilation rates

The optimization results of Strategy 1 are illustrated in Figure 5. The mechanisms behind the optimal ventilation strategy are clarified as follows. Firstly, the air change rate (ACH) in the first occupancy segment is reduced relative to the baseline scenario. This reduction may be attributed to the absence of initial airborne quanta, which slows the increase in quanta concentration, therefore allowing for reductions in ventilation and enhanced energy conservation. Secondly, the ACH in the final occupancy segments is lowered, which may be due to the higher quanta concentrations towards the end, hence does not substantially elevate the risk of infection, therefore allowing for decreased ventilation. Additionally, the ACH for the middle segments is optimized to maintain a relatively stable quanta concentration. Specifically, ACH in the middle break segments is greatly reduced, whereas ACH in the middle occupancy segments is increased compared to the baseline. Overall, the above adjustment strategically maximizes the combined benefits of break periods and outdoor ventilation to minimize quanta exposure and energy usage effectively. Increasing ACH during occupancy segments could compromise the effectiveness of breaks in reducing quanta levels, leading to unnecessary energy usage. Conversely, low ACH during occupancy segments could result in high initial quanta levels during break segments, necessitating increased ACH during break segments and thus leading to elevated energy consumption.

Furthermore, the optimized ventilation schedule adapts to outdoor weather conditions. Ventilation during the afternoon segments (post-lunch break) is slightly higher than during the morning segments (pre-lunch break). This discrepancy becomes more pronounced when comparing the last occupancy segment with the first one. This variation is due to more favorable outdoor conditions in the afternoon than in the morning for heating, with higher temperatures and lower relative humidity (RH), as shown in Figure 3, which contributes to reduced ventilation energy consumption.

3.1.2 Strategy 2 - constant ventilation rate but varying occupant schedules

Figure 6 presents the optimization results for Strategy 2, in which the durations of both occupancy and break segments vary within their predefined ranges. Significant changes compared to the base case can be observed in the optimal occupant schedule. Firstly, while the accumulated occupancy time remains equal to the base case, the total duration of the whole occupant schedule is notably shortened. This reduction primarily results from the strategic minimization of break periods. By carefully managing the lengths of each segment, the efficacy of break periods in reducing quanta concentration is enhanced, thereby allowing for a reduction in break time. Secondly, the occupant schedule is noticeably shifted later within the designated time zone (9:00–16:00). This adjustment is a strategic response to outdoor weather conditions, aiming to optimize energy conservation. The shortened schedule also increases the flexibility to modify the temporal distribution of the occupancy periods within this time zone.

Following this optimized schedule, the pattern of quanta concentration variation aligns with that observed in the base case, as depicted in Figure 1. This pattern is characterized by an increase in quanta concentration during occupancy segments and a decrease during break segments,

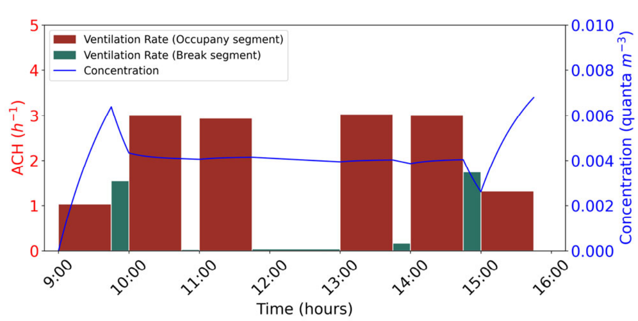

Fig. 5 Optimized ACH, fixed occupant schedule, and corresponding quanta concentration for Strategy 1

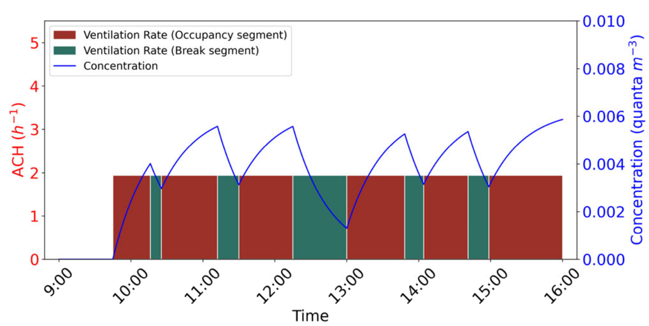

Fig. 6 Constant ACH, optimized occupant schedule, and corresponding quanta concentration for Strategy 2

demonstrating the effectiveness of the strategic adjustments made in Strategy 2.

3.1.3 Strategy 3 - varying ventilation rate and occupant schedule (consistent among segments)

The optimization results for Strategy 3 are illustrated in Figure 7. This strategy exhibits a pattern of quanta concentration variation similar to that in both the base case and Strategy 2, with quanta concentration increasing during occupancy segments and decreasing during break segments. The energy-saving mechanisms of Strategy 3 are consistent with those in Strategies 1 and 2 to a certain extent. Firstly, mirroring Strategy 1, Strategy 3 substantially reduces outdoor ventilation during the lunch break segment as an energy-saving measure. Secondly, akin to Strategy 2, Strategy 3 adjusts the time distribution of the entire occupant schedule with a rightward shift within the time zone (9:00–16:00) to take advantage of more favorable weather conditions in the afternoon. Additionally, following the approach of Strategy 2, Strategy 3 shortens the total duration of the occupant schedule by minimizing the cumulative break times. With the integrated approach of combining ventilation strategies, Strategy 3 is likely to accomplish a more substantial reduction in the accumulated break time compared to Strategy 2.

3.1.4 Strategy 4 - varying ventilation rate and occupant schedule

Figure 8 illustrates that Strategy 4 adopts a ventilation pattern similar to that of Strategy 1. Specifically, the strategy notably reduces outdoor ventilation during the first and last occupancy segments as well as the lunch break segment, while enhancing it during other occupancy segments to limit the accumulated quanta exposure. This similar ventilation schedule pattern leads to a similar trend in quanta concentration variations as Strategy 1, characterized by a significant increase in quanta concentration during the first and last occupancy segments, a notable decrease during the first and last break segments, and relative stability in

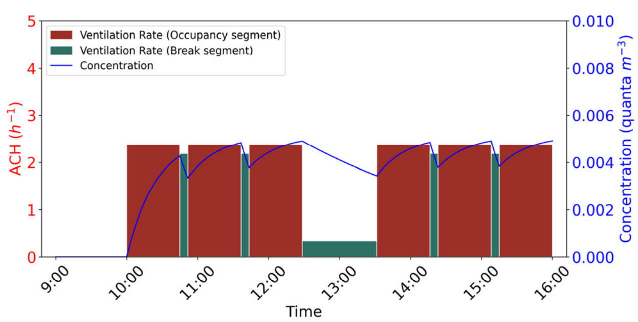

Fig. 7 Optimized ACH, optimized occupant schedule, and corresponding quanta concentration for Strategy 3

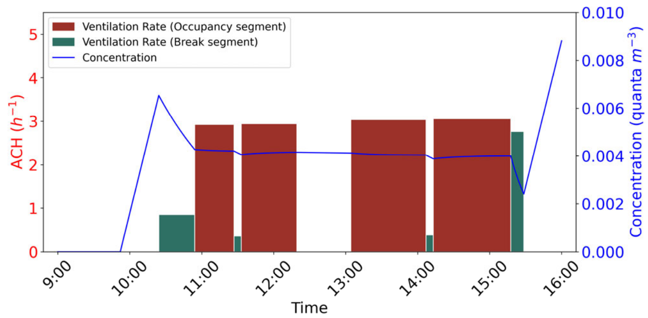

Fig. 8 Optimized ACH, optimized occupant schedule, and corresponding quanta concentration for Strategy 4

the other intermediate segments. Moreover, the optimized occupant schedule in Strategy 4 aligns with the energy-saving principles of Strategy 2, presenting a minimized and strategically time-shifted schedule. Importantly, the integration of occupant schedule management can enable Strategy 4 to attain a more substantial reduction in outdoor ventilation for the start, last, and lunch break segments compared to Strategy 1, resulting in further energy conservation.

3.1.5 Application potentials in real world scenarios

The selection of suitable control variables (i.e., ventilation and/or occupant schedule) in practice should consider a balance between energy-saving potential and practical applicability. More flexible adjustments of variables may offer greater energy savings but could also present challenges in application. Dynamically adjusting ventilation requires precise control, which could impact system longevity and reliability (Liu et al. 2022; Niu and Zhang 2023). Similarly, dynamic changes in occupancy durations could complicate scheduling and affect productivity, challenging the stability of a predictable occupancy pattern (Melikov et al. 2020; Zhang et al. 2023c). Strategy 4 offers the highest energy-saving potential due to its flexibility in adjusting both ACH and occupant schedules, maximizing the benefits of both factors in minimizing energy consumption while reducing infection risk. However, it is the least practical. In contrast, although Strategy 3 also optimizes both ACH and occupant schedules, it is less energy-efficient than Strategy 4 due to its consistent optimization pattern. But with steady occupancy and ventilation patterns, Strategy 3 is more applicable than Strategy 4. Strategy 1, which optimizes ventilation only, is the second energy efficient strategy, suitable when the change of the occupant schedule is prohibited. On the other hand, although it is the least energy-efficient option, Strategy 2 is particularly suitable for scenarios where adjusting the building's occupant schedule is feasible, but modifying the ventilation system's operation is not. However, it should be noted that while periodically vacating the classroom effectively reduces airborne transmission, it may also disrupt normal classroom activities, as students typically remain in the classroom during breaks. Nevertheless, during a pandemic, controlling transmission risk may take precedence over maintaining regular classroom routines. In future research, it would be valuable to further explore the energy-saving potential of our exposure-based ventilation control strategy while accommodating typical classroom usage patterns.

3.2 Energy saving potential in different climates

In this section, we ran the simulations for a full matrix of the four proposed strategies across four representative cities, each located in a different climate zone in China. The energy-saving potential is illustrated in Figures 9 and 10. Figure 9 displays the total energy consumption over five school days in one week in different seasons, while Figure 10 depicts the total energy reduction relative to the base case. Overall, the four strategies achieve effective energy reduction ratios, with the most efficient strategy exceeding 30% reduction compared to the base case. The performance of different strategies remains relatively stable across various climate zones and seasons, indicating the effectiveness of these strategies in different environmental settings. Notably, Strategy 4 emerges as the most energy-efficient approach across these conditions, followed by Strategy 1, Strategy 3, and Strategy 2.

Figure 9 illustrates that the absolute energy savings from various strategies are proportional to the base case energy consumption, which is primarily influenced by the difference between indoor and outdoor thermal conditions. For instance, Strategy 4 in Harbin, with a higher base case energy consumption in winter than in summer, saves ~27,000 kJ in winter and ~2800 kJ in summer over five school days. This difference occurs because changes in ventilation or occupant schedules, such as reducing ventilation by 0.5 ACH, can result in greater absolute energy savings when the indoor-outdoor thermal condition difference is larger. This highlights the critical role of indoor-outdoor thermal condition difference in determining potential energy savings.

Figure 10 further shows that the energy reduction ratio of different strategies typically inversely correlates with the base case energy consumption. Lower base case energy consumption typically results in a higher energy reduction ratio, as seen in Guangzhou during winter with a 33% reduction using Strategy 4, compared to only 15% in Harbin (see Figure 9(d) with Figure 10(d)). This inverse relationship arises from the calculating method of energy reduction ratio, where the reduced energy is divided by the base case energy consumption, emphasizing the influence of the energy consumption of the base case. However, deviations exist, such as in Beijing during autumn, where despite a lower energy consumption of the base case compared to Guangzhou in winter (see Figure 9(b) and 9(d)), the reduction ratio is less than in Guangzhou (see Figure 10(b) and 10(d)). This can be attributed to a more significant variation in Guangzhou's winter outdoor thermal conditions,

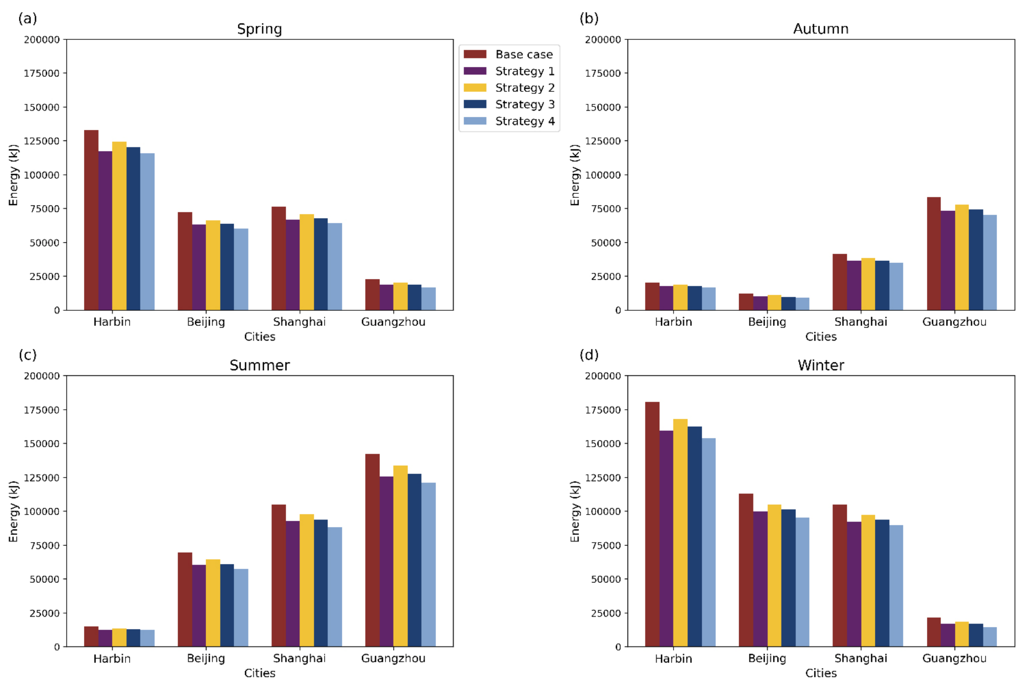

Fig. 9 Total energy consumption for schooling days in a week using different strategies across various cities and seasons: (a) spring, (b) autumn, (c) summer, and (d) winter

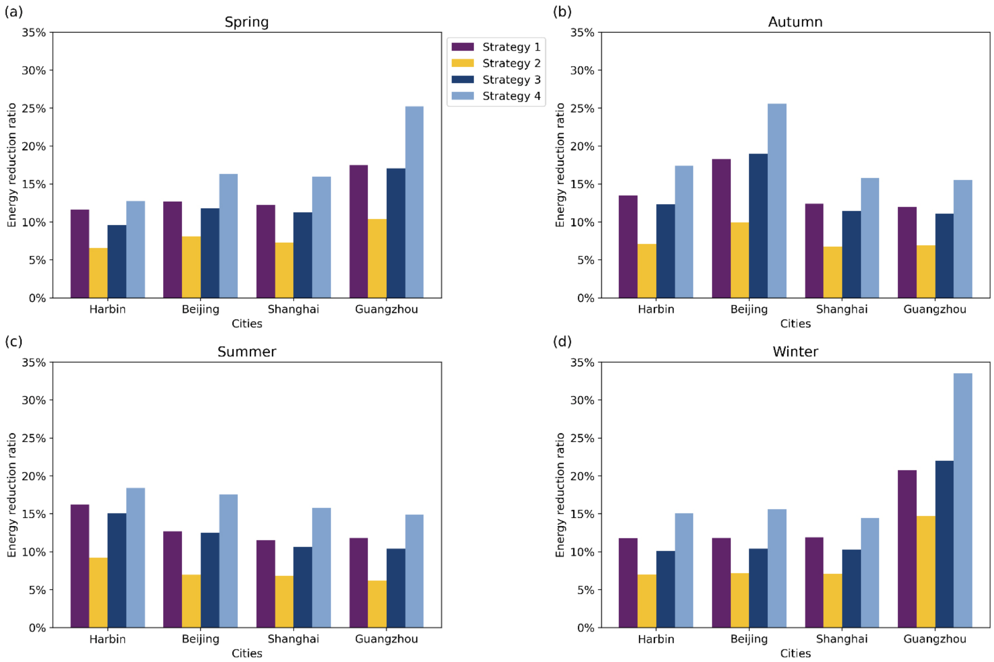

Fig. 10 Total energy reduction relative to the base case, measured over five consecutive school days and compared across different strategies, cities, and seasons: (a) spring, (b) autumn, (c) summer, and (d) winter

as detailed in the Supplementary Material. Such variability can enhance energy savings by leveraging more favorable weather conditions, underscoring the importance of both indoor-outdoor thermal differences and outdoor thermal condition variations in energy savings.

3.3 The impact of indoor thermal setpoints

The setpoints for maintaining indoor thermal conditions, including temperature and relative humidity, can significantly influence the base case energy consumption. Specifically, setting indoor thermal conditions vastly different from the outdoor conditions substantially increases the ventilation heating/cooling load. As established, for the proposed strategies, the quantity of reduced energy is proportional to the base case energy consumption level, indicating that varying indoor thermal condition setpoints can affect the energy reduction achieved.

Using Strategy 4 as an example, Figure 11 highlights how different indoor thermal condition setpoints affect (a) reduced energy consumption and (b) energy reduction ratio, compared to energy consumption at the same setpoint but without optimization, in Harbin during winter. Given Harbin's low temperature and relative humidity in winter, setpoints with higher temperature and relative humidity usually indicate a larger indoor-outdoor thermal condition difference, resulting in a higher heating load. The results in Figure 11 indicate that while increasing indoor temperature and relative humidity setpoints can enhance the quantity

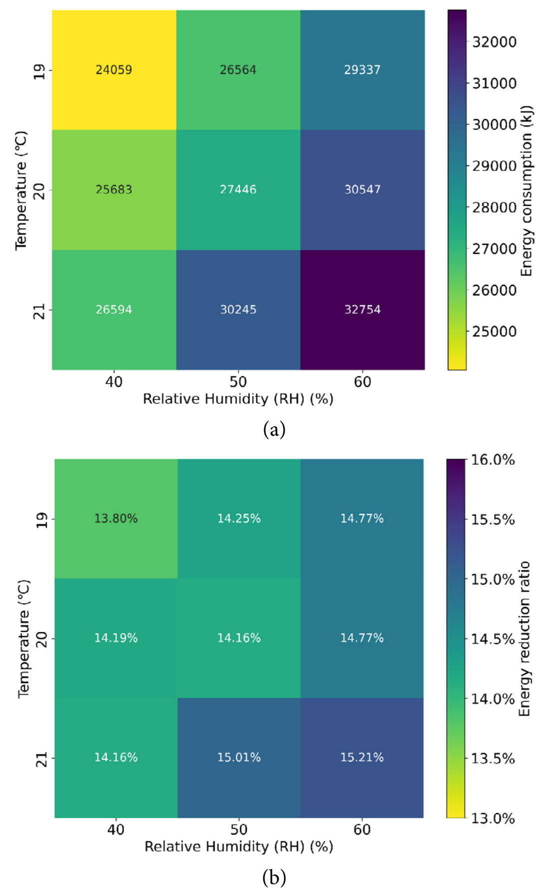

Fig. 11 (a) Energy reduced quantity and (b) energy reduction ratio achieved by Strategy 4 with different indoor thermal condition setpoints for Harbin in winter

of energy reduced, it only slightly improves the energy reduction ratio. Consequently, the total energy consumption at higher temperature and RH setpoints remains greater than at lower setpoints. This finding suggests that the reduced energy consumption achieved through the improved energy efficiency of the optimization strategy cannot compensate for the increased energy consumption due to the adjustment of indoor thermal condition setpoints. Therefore, indoor thermal condition setpoints should be carefully selected for energy conservation. Setpoints closer to outdoor thermal conditions are more effective in conserving energy.

3.4 Comparing with standard practice

Taking Strategy 4 as an example, Figure 12 further compares the energy efficiency of the proposed strategy with a standard practice (i.e., baseline occupant schedule and a ventilation rate of 10 L/s per person), which is widely recommended during the COVID-19 pandemic to ensure air quality and reduce the risk of virus transmission (EMG-SPI-B 2021; ASHRAE 2022; Li et al. 2022). The energy reduction ratio here refers to the total energy reduction (over five school days in one week) relative to the standard practice, with a higher reduction ratio indicating a higher energy efficiency.

Figure 12 shows that Strategy 4 achieves an energy reduction ratio of over 30% compared to the standard practice in all studied cases, with the maximum reduction reaching about 66% in Guangzhou during winter. These findings suggest that the standard ventilation rate of 10 L/s per person, while effective for minimizing transmission risks, can lead to excessive energy use. Rather than simply adopting a constant ventilation rate, new ventilation design methods and control strategies should be developed to not only maintain health and safety standards, but also optimize energy efficiency. Recent studies have proposed new ventilation design methods, which recommend deriving infection risk-based target ventilation rates for specific indoor spaces to save energy (Buonomano et al. 2023; Kurnitski et al. 2021, 2023).

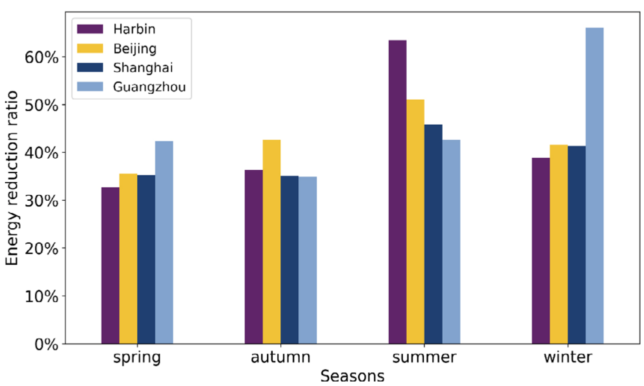

Fig. 12 Energy reduction ratio relative to the standard over five school days for Strategy 4, compared across various cities and seasons

Based on the exposure-based control theory we proposed, our results offer novel method to further enhance the energy efficiency of these infection risk-based ventilation design methods in school-like environments. This involves adjusting ventilation in response to outdoor weather conditions and incorporating suitable occupancy strategies, providing new perspectives for ventilation system design and operation.

4 Limitations and future work

Our study encompasses several limitations. First, the accuracy of our optimization algorithm requires further refinement. Given the large solution spaces, especially in Strategy 4 with over 20 decision variables, achieving precise analytical optimal solutions is computationally intensive and time-consuming. We use a metaheuristic approach, specifically the Genetic Algorithm (GA), to approximate the best solutions (Schmitt 2001; Lambora et al. 2019). However, the 'optimal' solutions from GA are approximations and not exact optima. The accuracy of these solutions heavily depends on the tuning of hyperparameters like population size, and the algorithm may converge on local optima. Adapting GA for specific scenarios such as varying classroom sizes and occupant capacities might require recalibration of these hyperparameters to enhance solution precision. In the future, more advanced methods, such as integrating GA with an Artificial Neural Network (ANN), can be further developed to efficiently predict and guide hyperparameter selection of GA.

Second, our optimization process only considers the heating/cooling load due to outdoor ventilation (Guo et al. 2022). However, a building's heating/cooling load is influenced by many factors, including internal loads and the building's thermal mass (Yang and Li 2008; Zeng et al. 2011; Hu and Karava 2014; Wang et al. 2014; Risbeck et al. 2021; Wu et al. 2023), which can be used with night ventilation to reduce cooling loads (Yang and Li 2008). Considering our main aim is to propose a novel ventilation and occupant control strategy for energy-efficient infection risk management, we have not included factors other than outdoor ventilation for simplicity and to reduce computational demands. Future studies can include a more comprehensive consideration of building energy consumption in the optimization process. In addition, our study primarily demonstrated the energy-saving potential of optimizing ventilation and occupant schedules for controlling long-range airborne transmission. However, other control measures, such as filtration, can also lower quanta concentrations in indoor air and should be considered as additional control variables in future investigations (Azimi and Stephens 2013; Fazli et al. 2019; Risbeck et al. 2021; Chang et al. 2023; Lyu et al. 2024; Yang et al. 2024; Yao et al. 2024).

Our results contain uncertainties associated with factors such as the estimation of quanta emission rates and the determination of risk thresholds. This study assumed a constant quanta emission rate; however, in reality, quanta emission rates can vary significantly due to factors such as individual differences and environmental conditions (Buonanno et al. 2020a, 2020b; Jones et al. 2021; Lyu et al. 2023; Lavor et al. 2025). The literature reports a wide range of quanta emission rates for classroom settings, from 0.37 quanta/h to 100 quanta/h (Buonanno et al. 2020a; Bazant and Bush 2021; Peng and Jimenez 2021). Such variability may influence optimization outcomes. Additionally, the selected risk threshold may jointly impact the energy-saving potential of the proposed strategies. For instance, a lower risk threshold and a higher quanta emission rate can lead to a lower limit for quanta exposure, necessitating higher outdoor ventilation. Consequently, the energy-saving potential from the dynamic adjustment of ventilation may be reduced, as a higher required average outdoor ventilation limits the feasibility of adjusting the ventilation rate in response to outdoor weather conditions. However, at the same time, the energy-saving potential from adjusting the occupant schedule may be enhanced, particularly since reducing energy consumption for the same duration is more effective at higher outdoor ventilation rates.

Moreover, in our study, both the occupant schedule and ventilation are optimized daily. However, frequently adjusting occupant schedules can be difficult in certain contexts. Instead, optimizing it based on averaged weather data over longer periods, such as seasonally, might be more feasible. In contrast, ventilation adjustments are generally more flexible. Optimizing ventilation based on daily weather predictions, rather than relying on averaged data over fixed periods, allows for greater adaptability to outdoor weather variations. Future studies could further enhance this adaptability by employing Rolling (Receding) Horizon Control methods. Such approaches would repeatedly optimize ventilation using real-time updated weather data, therefore improving responsiveness and overall performance (Kopanos and Pistikopoulos 2014; Ryzhov et al. 2019; Tabares-Velasco et al. 2019).

Finally, the energy-saving potential of the proposed optimization strategies depends heavily on the accuracy of outdoor weather predictions (Gholamzadehmir et al. 2020; Zhang et al. 2023a). This study utilized Typical Meteorological Years (TMY) weather files, representing averaged data predicting long-term climate variations. Future work could consider more accurate and detailed weather profiles, including localized or extreme weather predictions, to further explore the strategies' energy-saving potential (Han et al. 2021; Moazami et al. 2019). Additionally, this study considered climate data from only four climate zones, which may not fully capture global variations. Different weather conditions can lead to varying results, necessitating further investigation.

5 Conclusions

This study introduces innovative optimization strategies for controlling indoor long-range airborne transmission, by constraining total virus exposure rather than just concentration levels. Unlike traditional approaches that maintain quanta concentration below a fixed safe limit, our exposure-based control strategies allow quanta concentration to vary with time, enhancing flexibility in modifying occupant schedules and outdoor ventilation to optimize energy use. Based on it, we propose four distinct strategies to manage occupant schedule and ventilation within school environments, either individually or in combination, to balance infection risk with energy conservation.

The energy-saving potential of these strategies is two-fold. First, they allow for the adaptation of ventilation and occupant schedules to external weather conditions to maximize passive heating/cooling potential, thereby enhancing energy efficiency. For example, Strategy 1 adjusts air changes per hour (ACH) based on outdoor weather conditions, increasing ventilation during favorable weather conditions and reducing it when less favorable. Strategy 2 aligns the occupant schedule with optimal outdoor weather conditions, shifting occupancy to more favorable time. Second, the strategies permit adjustments in ACH or occupant schedules by considering their interaction, thus maximizing the combined benefits for reducing infection risks and conserving energy. An example of this is seen in Strategy 1, where ACH adjustments help maintain a stable quanta concentration across different segments, leveraging both break time and outdoor ventilation to reduce quanta levels efficiently and minimize overall energy usage.

Our results indicate that Strategy 4, which optimizes both the occupant schedule and ACH flexibly (with varying time durations for optimal segments and different ACH levels for each segment), is the most energy-efficient strategy, achieving energy reductions exceeding 30% compared to the baseline and over 60% relative to the standard ventilation scheme. This is followed by Strategy 1, which focuses solely on ACH, and Strategy 3, which optimizes both factors but in a stable manner (with uniform time durations and ACH levels for different types of segments). Strategy 2, focusing on optimizing only occupant schedule, is the least energy efficient, achieving only half the energy reduction of Strategy 1. The viability of these strategies has been proven across various climate zones and seasons, highlighting their broad applicability. Additionally, the significance of accurately establishing setpoints for indoor thermal conditions in the formulation of these optimization strategies has been affirmed, emphasizing the importance of a tailored approach.

Acknowledgements

Xiaowei Lyu acknowledged the financial support from China Scholarship Council (CSC) for pursuing her PhD at the University of Reading, UK.

Declaration of competing interest

The authors have no competing interests to declare that are relevant to the content of this article. Zhiwen Luo is a Subject Editor of *Building Simulation*.

Author contribution statement

Conceptualization: Xiaowei Lyu; Methodology: Xiaowei Lyu, Zhiwen Luo, Zhan Shu; Formal analysis and investigation: Xiaowei Lyu, Zhiwen Luo; Writing—original draft preparation: Xiaowei Lyu; Writing—review and editing: Xiaowei Lyu, Zhiwen Luo, Emmanuel Essah; Supervision: Zhiwen Luo, Emmanuel Essah, Li Shao.

References

Adams WC (1993). Measurement of breathing rate and volume in routinely performed daily activities. Los Angeles: University of California.

ASHRAE (2022). ASHRAE positions on infectious aerosols. Atlanta, GA, USA: American Society of Heating, Refrigerating and Air-Conditioning Engineers.

Azimi P, Stephens B (2013). HVAC filtration for controlling infectious airborne disease transmission in indoor environments: Predicting risk reductions and operational costs. *Building and Environment*, 70: 150–160.

Bazant MZ, Bush JWM (2021). A guideline to limit indoor airborne transmission of COVID-19. *PNAS*, 118: e2018995118.

Buonanno G, Morawska L, Stabile L (2020a). Quantitative assessment of the risk of airborne transmission of SARS-CoV-2 infection: Prospective and retrospective applications. *Environment International*, 145: 106112.

Buonanno G, Stabile L, Morawska L (2020b). Estimation of airborne viral emission: Quanta emission rate of SARS-CoV-2 for infection risk assessment. *Environment International*, 141: 105794.

Buonomano A, Forzano C, Giuzio GF, et al. (2023). New ventilation design criteria for energy sustainability and indoor air quality in a post Covid-19 scenario. *Renewable and Sustainable Energy Reviews*, 182: 113378.

Chang Y, Ai Z, Ye J, et al. (2023). A cost-effectiveness assessment of the operational parameters of central HVAC systems during pandemics. *Building Simulation*, 16: 667–682.

Dai H, Zhao B (2020). Association of the infection probability of COVID-19 with ventilation rates in confined spaces. *Building Simulation*, 13: 1321–1327.

EMG-SPI-B (2021). Application of CO_2 monitoring as an approach to managing ventilation to mitigate SARS-CoV-2 transmission. Environmental Modelling Group (EMG) and Scientific Pandemic Insights Group on Behaviours (SPI-B).

Fazli T, Zeng Y, Stephens B (2019). Fine and ultrafine particle removal efficiency of new residential HVAC filters. *Indoor Air*, 29: 656–669.

Feng Y, Fan Y, Luo X, et al. (2024). A Wells-Riley based COVID-19 infectious risk assessment model combining both short range and room scale effects. *Building Simulation*, 17: 93–111.

Gholamzadehmir M, Del Pero C, Buffa S, et al. (2020). Adaptive-predictive control strategy for HVAC systems in smart buildings—A review. *Sustainable Cities and Society*, 63: 102480.

Guo Y, Zhang N, Hu T, et al. (2022). Optimization of energy efficiency and COVID-19 pandemic control in different indoor environments. *Energy and Buildings*, 261: 111954.

Han JM, Ang Y, Malkawi A, et al. (2021). Using recurrent neural networks for localized weather prediction with combined use of public airport data and on-site measurements. *Building and Environment*, 192: 107601.

Henriques A, Jia W, et al. (2025). An integrated airborne transmission risk assessment model for respiratory viruses: Short- and long-range contributions. *Journal of the Royal Society Interface*, 22: 20240740.

Hu J, Karava P (2014). Model predictive control strategies for buildings with mixed-mode cooling. *Building and Environment*, 71: 233–244.

Jones B, Sharpe P, Iddon C, et al. (2021). Modelling uncertainty in the relative risk of exposure to the SARS-CoV-2 virus by airborne aerosol transmission in well mixed indoor air. *Building and Environment*, 191: 107617.

Kopanos GM, Pistikopoulos EN (2014). Reactive scheduling by a multiparametric programming rolling horizon framework: A case of a network of combined heat and power units. *Industrial & Engineering Chemistry Research*, 53: 4366–4386.

Kurnitski J, Kiil M, Wargocki P, et al. (2021). Respiratory infection risk-based ventilation design method. *Building and Environment*, 206: 108387.

Kurnitski J, Kiil M, Mikola A, et al. (2023). Post-COVID ventilation design: Infection risk-based target ventilation rates and point source ventilation effectiveness. *Energy and Buildings*, 296: 113386.

Lambora A, Gupta K, Chopra K (2019). Genetic algorithm - A literature review. In: Proceedings of the 2019 International Conference on Machine Learning, Big Data, Cloud and Parallel Computing, Faridabad, India, pp. 380–384.

Lavor V, Wei J, Coceal O, et al. (2025). Quanta emission rate during speaking and coughing mediated by indoor temperature and humidity. *Environment International*, 198: 109379.

Li Y (2021). Basic routes of transmission of respiratory pathogens—A new proposal for transmission categorization based on respiratory spray, inhalation, and touch. *Indoor Air*, 31: 3–6.

Li Y, Qian H, Hang J, et al. (2021). Probable airborne transmission of SARS-CoV-2 in a poorly ventilated restaurant. *Building and Environment*, 196: 107788.

Li B, Cai W (2022). A novel CO_2-based demand-controlled ventilation strategy to limit the spread of COVID-19 in the indoor environment. *Building and Environment*, 219: 109232.

Li Y, Cheng P, Jia W (2022). Poor ventilation worsens short-range airborne transmission of respiratory infection. *Indoor Air*, 32: e12946.

Li B, Wang S, Li X (2024). A practical real-time control strategy for high-performance building HVAC operation concerning potential pandemic outbreaks in post-pandemic era. *Building and Environment*, 263: 111856.

Liu Z, Xie Y, Hu X, et al. (2022). A control strategy for cabin temperature of electric vehicle considering health ventilation for lowering virus infection. *International Journal of Thermal Sciences*, 172: 107371.

Lyu X, Luo Z, Shao L, et al. (2023). Safe CO_2 threshold limits for indoor long-range airborne transmission control of COVID-19. *Building and Environment*, 234: 109967.

Lyu X, Luo Z, Shao L (2024). Size dependent effectiveness of engineering and administrative control strategies for both short- and long-range airborne transmission control. *Environmental Science: Atmospheres*, 4: 43–56.

Melikov AK, Ai ZT, Markov DG (2020). Intermittent occupancy combined with ventilation: An efficient strategy for the reduction of airborne transmission indoors. *Science of The Total Environment*, 744: 140908.

Miller SL, Nazaroff WW, Jimenez JL, et al. (2021). Transmission of SARS-CoV-2 by inhalation of respiratory aerosol in the Skagit Valley Chorale superspreading event. *Indoor Air*, 31: 314–323.

Moazami A, Nik VM, Carlucci S, et al. (2019). Impacts of future weather data typology on building energy performance—Investigating long-term patterns of climate change and extreme weather conditions. *Applied Energy*, 238: 696–720.

Mokhtari R, Jahangir MH (2021). The effect of occupant distribution on energy consumption and COVID-19 infection in buildings: A case study of university building. *Building and Environment*, 190: 107561.

Morawska L, Allen J, Bahnfleth W, et al. (2024). Mandating indoor air quality for public buildings. *Science*, 383: 1418–1420.

Nie J, Yuan S, Fang L, et al. (2018). Experimental study on an innovative enthalpy recovery technology based on indirect flash evaporative cooling. *Applied Thermal Engineering*, 129: 22–30.

Niu D, Zhang S (2023). Outdoor thermal condition based-segmented intermittent demand-controlled ventilation for constant-air-volume system. *Building and Environment*, 244: 110815.

Pang Z, Lu X, O'Neill Z (2023). Quantification of how mechanical ventilation influences the airborne infection risk of COVID-19 and HVAC energy consumption in office buildings. *Building Simulation*, 16: 713–732.

Peng Z, Jimenez JL (2021). Exhaled CO_2 as a COVID-19 infection risk proxy for different indoor environments and activities. *Environmental Science & Technology Letters*, 8: 392–397.

Peng Z, Rojas ALP, Kropff E, et al. (2022). Practical indicators for risk of airborne transmission in shared indoor environments and their application to COVID-19 outbreaks. *Environmental Science & Technology*, 56: 1125–1137.

Riley EC, Murphy G, Riley RL (1978). Airborne spread of measles in a suburban elementary school. *American Journal of Epidemiology*, 107: 421–432.

Risbeck MJ, Bazant MZ, Jiang Z, et al. (2021). Modeling and multiobjective optimization of indoor airborne disease transmission risk and associated energy consumption for building HVAC systems. *Energy and Buildings*, 253: 111497.

Risbeck MJ, Cohen AE, Douglas JD, et al. (2023). Data-driven control of airborne infection risk and energy use in buildings. *Building and Environment*, 245: 110893.

Ryzhov A, Ouerdane H, Gryazina E, et al. (2019). Model predictive control of indoor microclimate: Existing building stock comfort improvement. *Energy Conversion and Management*, 179: 219–228.

Schmitt LM (2001). Theory of genetic algorithms. *Theoretical Computer Science*, 259: 1–61.

Sha H, Zhang X, Qi D (2021). Optimal control of high-rise building mechanical ventilation system for achieving low risk of COVID-19 transmission and ventilative cooling. *Sustainable Cities and Society*, 74: 103256.

Tabares-Velasco PC, Speake A, Harris M, et al. (2019). A modeling framework for optimization-based control of a residential building thermostat for time-of-use pricing. *Applied Energy*, 242: 1346–1357.

Wang X, Cheng R, Zeng R, et al. (2014). Ideal thermal physical properties of building wall in an active room. *Indoor and Built Environment*, 23: 839–853.

Wei J, Li Y (2016). Airborne spread of infectious agents in the indoor environment. *American Journal of Infection Control*, 44: S102–S108.

Wei L, Liu G, Yuan Y, et al. (2023). A framework for airborne infection risk assessment based on real-time occupant distribution prediction in outpatient waiting space. *Journal of Building Engineering*, 76: 107109.

Wu W, Benner J, Luo Z (2023). Developing analytical model for nighttime cooling of internal thermal mass. *Applied Thermal Engineering*, 220: 119798.

Yang L, Li Y (2008). Cooling load reduction by using thermal mass and night ventilation. *Energy and Buildings*, 40: 2052–2058.

Yang G, Wang Y, Chan KC, et al. (2024). Effectiveness of air cleaner on mitigating the transmission of respiratory disease in a dental clinic environment. *Building Simulation*, 17: 1789–1803.

Yao G, Liu Z, Shi J, et al. (2024). Comprehensive evaluations of the bioaerosol filtration performance of high- and medium-efficiency filters under different influencing factors. *Building Simulation*, 17: 2249–2262.

Zeng R, Wang X, Di H, et al. (2011). New concepts and approach for developing energy efficient buildings: Ideal specific heat for building internal thermal mass. *Energy and Buildings*, 43: 1081–1090.

Zhang S, Ai Z, Lin Z (2021). Occupancy-aided ventilation for both airborne infection risk control and work productivity. *Building and Environment*, 188: 107506.

Zhang L, Chen Z, Zhang X, et al. (2023a). Challenges and opportunities of machine learning control in building operations. *Building Simulation*, 16: 831–852.

Zhang N, Hu T, Niu M, et al. (2023b). Building energy efficiency and COVID-19 infection risk: Lessons from office room management. *Building Simulation*, 16: 1425–1438.

Zhang S, Niu D, Lin Z (2023c). Occupancy-aided ventilation for airborne infection risk control: Continuously or intermittently reduced occupancies? *Building Simulation*, 16: 733–747.

Zheng W, Hu J, Wang Z, et al. (2021). COVID-19 impact on operation and energy consumption of heating, ventilation and air-conditioning (HVAC) systems. *Advances in Applied Energy*, 3: 100040.

Zhuang C, Choudhary R, Mavrogianni A (2022). Probabilistic occupancy forecasting for risk-aware optimal ventilation through autoencoder Bayesian deep neural networks. *Building and Environment*, 219: 109207.

Supplementary Material

1. Outdoor thermal conditions of studied cases

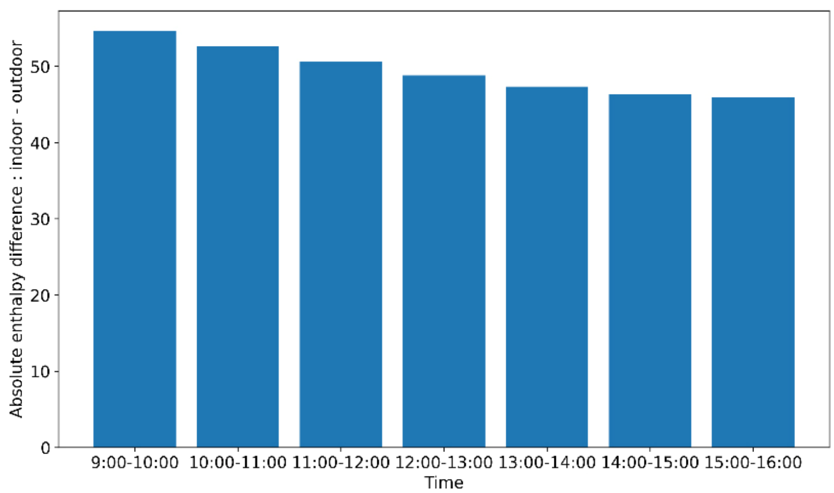

Fig. S1 Average values of the 5 consecutive days for Harbin during winter

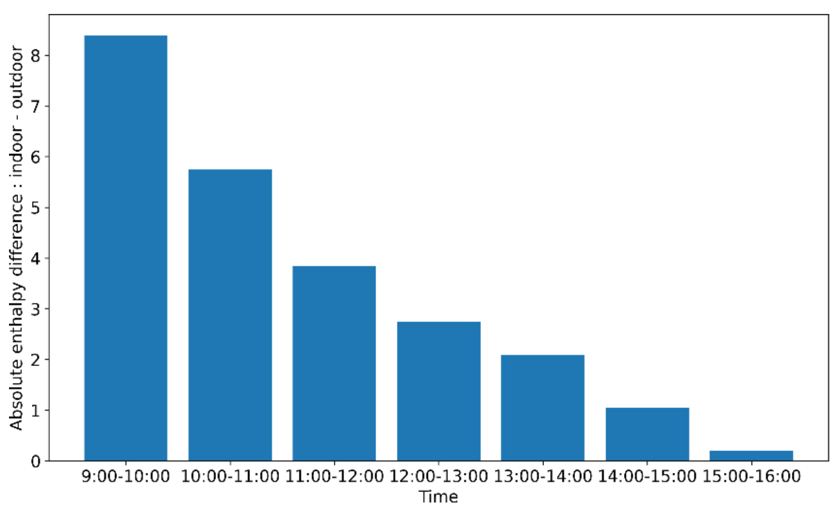

Fig. S2 Average values of the 5 consecutive days for Guangzhou during winter